Comparison of chain versus sheet crystal structures for the cyanides MCN (M=Cu—Au) and dicarbides MC_2 (M=Be—Ba,Zn—Hg)

P. Zaleski-Ejgierd,[1] M. Hakala,[2] and P. Pyykkö[1,*]

[1]*Laboratory for Instruction in Swedish, Department of Chemistry, University of Helsinki, P.O. Box 55, FIN-00014, Helsinki, Finland*

[2]*Division of X-ray Physics, Department of Physical Sciences, University of Helsinki, P.O. Box 64, FIN-00014, Helsinki, Finland*

(Received 26 January 2007; revised manuscript received 20 April 2007; published 10 September 2007)

The cyanides MCN, M=Cu,Ag,Au, have experimentally a structure with hexagonally packed, infinite —M—CN—M—CN— chains. Following our earlier study for AuCN, we now predict that all three MCN could have an alternative $M_3C_3N_3$ sheet structure of comparable energy with the known one. The valence isoelectronic systems MC_2 versus M_3C_6, M=Be—Ba,Zn—Hg, are also studied. Now, the known dicarbides have the CaC_2 or MgC_2 chain structures, which are well reproduced. The predicted sheets lie energetically below the chains for M=Zn, Cd, and Hg. All these group-12 systems are experimentally unknown. Indeed, they are clearly endothermic, compared to the elements. For some sheet structures, the densities of states suggest rather small band gaps and even metallic character. When available, the experimental geometries agree well with the calculated ones.

DOI: 10.1103/PhysRevB.76.094104 PACS number(s): 61.50.Ah, 61.66.−f, 33.15.Dj, 78.70.Ck

I. INTRODUCTION

One of the fundamental goals of computational materials science is the prediction of new chemical species and the determination of their properties.[1] A recent example is gold cyanide, AuCN, a well-known commodity chemical, whose known structure consists of infinite —CN—Au—CN—Au— chains.[2] The chains are packed together on a hexagonal grid in such a way that the Au atoms are in the same plane [see Fig. 1(A′)]. However, Hakala and Pyykkö[3] recently predicted for AuCN an alternative crystal structure, having a closely similar energy but only ~70% of the density [see Fig. 1(B′)]. The new structure contains triazine-type six rings of three carbon and three nitrogen atoms, C_3N_3, which are coupled to each other by linearly coordinated gold(I) atoms forming a two-dimensional sheet structure. The sheets attract each other weakly due to the gold-gold aurophilic interaction. Such a new structure has not yet been observed. Since single-sheet-type two-dimensional (2D) atomic crystals, such as graphene, are potentially a very important class of materials but much less known than the three-dimensional (3D) counterparts,[4] it is interesting to ask whether such a structure could also be found for other similar systems, such as the cyanides involving the other group-11 (coinage) metals, namely, copper and silver. Their known crystalline structure is also chain type: —CN—M—CN—M— (M denoting the metal).[5–7]

By applying the valence isoelectronic principle, one can extend the search for new sheet-type structures to further cases. Replacing the formula MCN of the metal cyanides by the formula MC_2, with an $(ns)^2$ configuration for the neutral metal atom M, leads to the class of crystalline dicarbides. Metallic dicarbides may have interesting electronic properties, such as the superconductivity of YC_2 and its layered compounds.[8] In the present work, we have studied metallic elements in groups 2 (alkaline earth metals M=Be, Mg, Ca, Sr, and Ba) and 12 (transition metals M=Zn, Cd, and Hg). Stable crystalline structures are known only for some of these systems (MgC_2,CaC_2,SrC_2,BaC_2). No earlier data were found for any group-12 dicarbides. The previously known crystal structures of CaC_2, SrC_2, and BaC_2 from group 2 consist of infinite —M—CC—M—CC— chains, but each cation is now equatorially surrounded by four anions, each parallel to the z axis [see Fig. 2(B)]. Another known group-2 dicarbide, MgC_2, also has infinite chains, but the four equatorial dicarbide ligands around the cation are now perpendicular to the z axis [see Fig. 2(C)]. These structures have been only very recently clarified by x-ray and neutron diffraction.[9–12]

In the present work, we show that sheet-type structures, such as the recently reported[3] poly(triaurotriazine) for AuCN, can also be found for the other group-11 coinage metal cyanides and for group-2 and -12 dicarbides. For group-12 dicarbides and for BeC_2 of group 2, we also investigate whether they could form stable structures in the tetragonal geometry starting the search from the experimental geometry known for group 2. An earlier crystal-Hartree-Fock calculation for CaC_2 reproduced well the experimental structure.[13] We have performed density of states (DOS) analysis for both isolated and packed structures, and discuss the insulator vs metallic properties of the studied systems. The vibrational frequencies at the center of the Brillouin zone have been calculated to provide tools for the identifica-

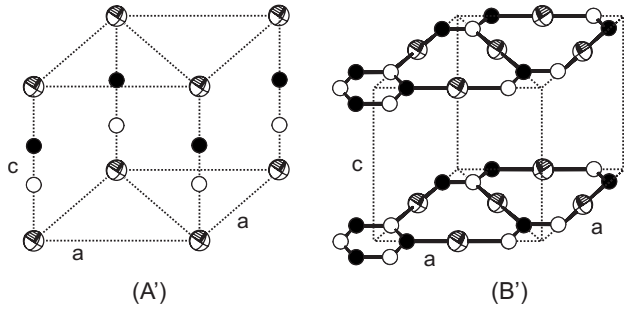

FIG. 1. Investigated crystal structures for group-11 metal cyanides (M, spheres; C, black circles; N, white circles): (A′) chain structure MCN ($P6mm$) and (B′) sheet structure $M_3C_3N_3$ ($P\bar{6}2m$).

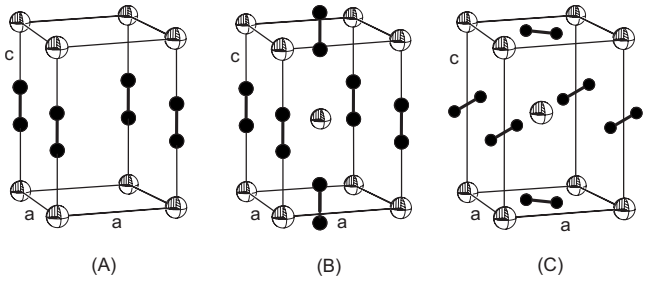

FIG. 2. Investigated crystal structures for chain-type metal dicarbides MC_2 (M, spheres; C, black circles): (A) tetragonal ($P4/mmm$), (B) tetragonal ($I4/mmm$), and (C) tetragonal ($P4_2/mmm$).

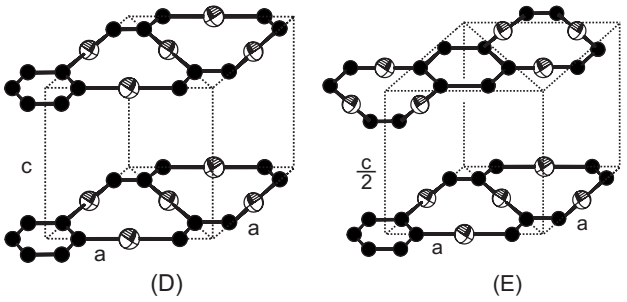

FIG. 3. Investigated crystal structures for sheet-type metal dicarbides M_3C_6 (M, spheres; C, black circles): (D) simple stacking ($P\frac{6}{m}mm$) and (E) shifted ($P\bar{6}2m$).

tion. The geometries and frequencies are compared to the known cyanide and dicarbide results. Finally, the thermodynamical preferences of the predicted dicarbides are estimated by calculating their formation energies with respect to the elemental metals and graphite as starting materials.

II. METHOD

All calculations were performed within density functional theory (DFT) using the Vienna *ab initio* simulation package[14–16] (VASP). Plane-wave basis sets and projector augmented-wave potentials[17,18] with the generalized gradient approximation[19] (GGA) for the Perdew-Burke-Ernzerhof[20] exchange-correlation functional were employed. When optimizing the lattice parameters and the atomic positions, constant-volume calculations were performed with the symmetry of the unit cell kept fixed. We typically scanned the crystal volume for each system by changing the interchain or intersheet distance in steps of 0.1 Å and letting the system relax. In this work, we will report the energy value and the atomic geometry corresponding to the minimum point on the total energy curve for each system.

For the energy cutoff, we used a standard 400 eV value. A Γ-centered $6\times6\times6$ k-point grid was used throughout the work for the lattice optimizations and vibrational frequencies at the Γ point of the Brillouin zone. All the chain structures and the majority of the sheet structures studied were found to be insulators, and this choice of the k-point grid was found sufficient for the convergence in total energy and geometry. For the dynamical matrix and vibrational frequencies, a shift of 0.025 Å was applied to the atomic positions. Some sheet structures exhibited the closing of the band gap as the sheets were packed together, and two dicarbides were manifestly metallic already as isolated sheets. The semimetallic vs metallic character for these systems was inferred by studying the DOS at the Fermi level. For the systems with a small band gap, the used k-point grid may lead to a slight overestimation of the total energy (~0.005 eV) and the sheet-sheet distance (~0.2 Å), as compared with the calculations using denser k-point grids. We expect a similar behavior also for the two metallic systems. In our tests, the intrachain and intrasheet distances C—N, M—C, and M—N were well converged within 0.2% with respect to increasing the k-point grid above that of $6\times6\times6$. When the dispersion interactions are the dominant mechanism, such as in the case of interchain distances in cyanides, the present DFT-GGA results are not expected to be reliable and should be considered with caution.

The studied geometries are illustrated in Figs. 1–4. We refer to the geometries as "chains" [see Figs. 1(A′) and 2(A)–2(C)] and to the rest as "sheets." Furthermore, it turned out to be necessary to consider four different packings of the sheets: "simple stacking," where each 2D sheet is simply repeated in the perpendicular direction to form the 3D crystal [see Figs. 1(B′) and 3(D)]; "shifted," where every second 2D sheet is parallelly displaced, so that the benzenelike carbon ring lies on top of the "triangle" formed by the metal atoms [see Fig. 3(E)]; "rotated," the same as simple stacking but the carbon ring is rotated inside the sheet with respect to the connecting metals by 30° [see Fig. 4(F)]; "shifted+rotated," where in addition to the rotated structure, there is also the displacement parallel to the plane as described above [see Fig. 4(G)].

III. RESULTS AND DISCUSSION

A. Geometries and total energies

1. Cyanides MCN

The properties of the studied coinage metal cyanides CuCN, AgCN, and AuCN are found to be very similar con-

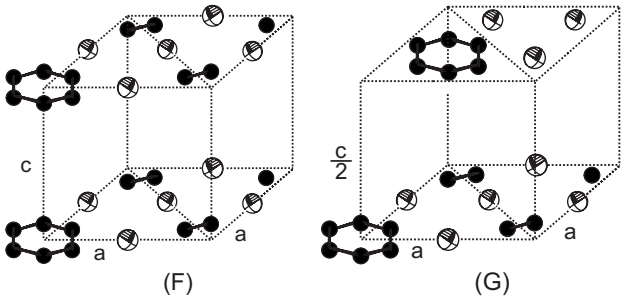

FIG. 4. Investigated crystal structures for sheet-type metal dicarbides M_3C_6 (M, spheres; C, black circles): (F) rotated ($P\frac{6}{m}mm$) and (G) rotated plus shift ($P\bar{6}2m$).

TABLE I. Total energy difference ΔE (eV) between the chain and sheet structures for group-11 metal cyanides (per *M*CN formula unit). Both 3D and isolated cases are reported. Negative value indicates that the chain structure is more stable.

Case	CuCN	AuCN	AuCN
3D sheet vs 3D chain	−0.22	−0.18	0.00
2D sheet vs 1D chain	−0.24	−0.21	0.03

cerning geometries and total energies. Like in the case of AuCN,[3] our simulations reproduce, for the two other compounds, the experimentally known geometry within the chain and predict the possible existence of a sheet-type structure. The chain-type structure of AgCN and CuCN is known to differ from that of AuCN due to an even weaker chain-chain interaction. In the case of AuCN, the aurophilic interaction keeps the interchain structure to a large extent ordered (sixfold *P*6*mm* symmetry about the chain axis), whereas in the two other cases there is a considerable degree of disorder, leading to a lower threefold symmetry.[5–7] For the present analysis, all the chain-type structures were confined to the *P*6*mm* symmetry [Fig. 1(A′)]. This is well sufficient for the description of the strong covalent bonds C—N, *M*—C, and *M*—N within the chains. The interchain search geometry for CuCN and AgCN is not the one experimentally suggested but, as the attraction between the chains is due to dispersion, DFT-GGA is not expected to perform correctly for this distance in any case.

For the $M_3C_3N_3$ sheet structures, a total energy minimum was found for the simple stacking geometry [see Fig. 1(B′)] with symmetry $P\bar{6}2m$, whereas no stable structures were found corresponding to the other sheet geometries. The total energies for the chain and sheet structures are compared in Table I. The energy differences are about 0.2 eV for CuCN and AgCN, but for AuCN there is practically no difference between the two structures. Due to the weak sheet-sheet and chain-chain interactions, the comparison of the isolated structures leads to the same conclusion.

Table II gives the bond lengths and the lattice constants, along with the experimental values for the known *M*—N, *M*—C, and C—N distances. We compare our results with the experimental values from Hibble *et al.*,[6,7,21] who performed a systematic total neutron diffraction study for these structures. Their results differ somewhat from the conventional Bragg scattering studies, which, according to them, do not yield completely satisfactory results. For the chain structures, the experimental intrachain covalent bond lengths are very well described with distances accurate to 2% or better. In particular, the C—N distance is well reproduced. The difference between the *M*—C and *M*—N bond lengths in sheets compared to the same difference in chains is larger. For sheets, the C—N bond lengths are practically the same for all the cyanides, but larger by about 20 pm compared to the chain structure, reflecting the aromatic six-ring bonding as contrasted to the —C≡N— triple bonds.

Because of the well-known difficulties in describing dispersion effects by DFT, the interchain and intersheet distances should be considered much more uncertain, which can be seen in the large theory-experiment discrepancy of the lattice parameter *a* for AuCN, which for this system corresponds to the chain-chain distance. The comparison of the interchain distances with the experimental values is further complicated, because the chains are randomly displaced along the chain axis, and for AgCN and CuCN there are no chemical bonds between the chains.[6,7,21] As a matter of fact, the latter is reflected in the very weak binding energy between the isolated and packed CuCN and AgCN chains in our calculations. The binding energy for isolated sheets re-

TABLE II. Bond lengths, lattice parameters *a* and *c* (pm), and volumes *V* (Å^3) for group-11 metal cyanides. The volume is given with respect to one *M*CN unit. The values *a* and *V* given in italics are not directly comparable to the experiment due to the different crystal symmetry in the calculation. The capital letter after the compound refers to the crystal structures in Fig. 1.

Chains	Source	*M*—C	*M*—N	C—N	*a*	*c*	*V*
CuCN (A′)	Calc.	182.0	181.9	117.4	*407.7*	481.2	*69.27*
	Expt.[a]	184.6	184.6	117.0	591.2(3)	486.107(3)	49.0467
AgCN (A′)	Calc.	201.9	204.0	117.0	*410.8*	523.9	*76.56*
	Expt.[b]	206	206	116	590.32	528.29	53.1443
AuCN (A′)	Calc.	194.3	198.3	116.8	379.4	511.3	63.74
	Expt.[c]	197.03(5)	197.03(5)	114.99(2)	340.5(4)	509.2(2)	51.1273
Sheet	Source	*M*—C	*M*—N	C—N	*a*	*c*	*V*
$Cu_3C_3N_3$ (B′)	Calc.	187.6	190.0	136.6	650.7	332.4	81.24
$Ag_3C_3N_3$ (B′)	Calc.	207.4	213.8	136.1	693.3	341.5	94.78
$Au_3C_3N_3$ (B′)	Calc.	199.5	210.4	136.3	682.5	352.4	94.78

[a]Reference 7.
[b]Reference 6.
[c]Reference 21.

TABLE III. Experimental and calculated lattice parameters a and c (pm), cell volumes V (Å^3), symmetries, and bond lengths (pm) for group-2 metal dicarbides in the chain structure. Volume is given with respect to one MC_2 unit. The capital letter after the compound refers to the crystal structures in Fig. 2.

	BeC_2 (B)	MgC_2 (C)		CaC_2 (B)		SrC_2 (B)		BaC_2 (B)	
	Calc.	Calc.	Expt.[a]	Calc.	Expt.[b]	Calc.	Expt.[c]	Calc.	Expt.[d]
Lattice constant a	390.6	396.9	393.42(7)[a]	391.3	388.582(4)[b]	414.4	411.43(2)[c]	440.6	439.43(6)[d]
Lattice constant c	463.2	492.5	502.1(1)	640.0	640.05(1)	681.8	676.60(4)	724.1	712.5(2)
Volume V	35.01	38.8	38.85	49.0	48.20	58.60	57.26	70.3	68.88
Symmetry	$I4/mmm$	$P4_2/mnm$		$I4/mmm$		$I4/mmm$		$I4/mmm$	
				Bond lengths					
Chain-chain dist.	276.1	280.6	278.2	276.7	274.7	293.0	290.8	311.6	310.7
M—C	169.1	217.8	217.4	256.8	255.2(4)	277.7	278.5(8)	298.8	297.0(7)
C—C	124.9	125.8	121.5	126.4	129.7(8)	126.4	120(2)	126.6	118.6(13)
				123.9[e]					

[a]Reference 9.
[b]Reference 25.
[c]Reference 10.
[d]Reference 11.
[e]HF level, Ref. 13.

quired to form a 3D structure is found to be typically 0.05 eV.

It is interesting to note that room-temperature powder-x-ray pattern for CuCN shows unexplained weak Bragg peaks at distances d_1=260.5 pm and d_2=235.3 pm (Ref. 7). These have been attributed to an unknown highly crystalline form β-CuCN with density of 2.97 g cm^{-3} (cf. 3.03 g cm^{-3} for the known α-CuCN). Whether such peaks could be correlated with our predicted sheet-type geometry or its modifications remains an open question. The crystal density of the sheet structure is 1.8 g cm^{-3}, i.e., ~40% smaller than that assigned to β-CuCN.

2. Dicarbides MC_2

The geometries of the metal dicarbides in the known experimental chain structure (M=Mg—Ba in group 2) are well reproduced by our calculations. In addition, also for the dicarbides we predict the possible existence of sheet structures for both groups 2 and 12, and for group 12 we find possible chain structures. Experimentally, group-2 dicarbides crystallize in two different tetragonal symmetries, viz., $I4/mmm$ for MC_2 (M=Ca—Ba) and $P4_2/mnm$ for MgC_2. Table III contains the calculated bond lengths and lattice parameters for group-2 chain dicarbides in comparison with the available experimental data. Table IV contains the predictions for chain structures for group 12.

For the known group-2 dicarbides in the chain structure, the calculated covalent bond lengths are in good agreement with experiment. Our calculations systematically give slightly larger values of the C—C bond length (around 125 pm) compared to the experimental results (around 120 pm), the C—C bond length in acetylene molecule[22] (120.4 pm) or the bond length calculated from the carbon triple-bond covalent radius (120 pm).[23] We have checked that our calculation for the acetylene molecule gives a triple-bond length of 120.8 pm in good agreement with experiment. Therefore, the use of GGA may not necessarily explain the higher dicarbide C—C lengths compared to the measured ones. Instead, a possible reason for the difference could be the vibrational motion of the dicarbide group in the experiments.[9] In realistic physical conditions, when thermal energy is applied, C_2^{2-} group can both librate and vibrate,[13] thus leading to an underestimation of the C—C bond length by experimental measurement. No quantitative data for the shortening of the apparent C—C distance are available. Zibrowius *et al.*[24] do give NMR values for the amplitude of the rotational vibrations of the C_2^{2-} dumbbells in K_2C_2. An interesting point to notice is that for ZnC_2, CdC_2, and HgC_2, we predict the possible existence of a chain structure in the $I4/mmm$ geometry similar to the MC_2 (M=Ca—Ba) structures. The $P4_2/mnm$ geometry for ZnC_2, CdC_2, and HgC_2 was also

TABLE IV. Calculated lattice parameters a and c (pm), cell volumes V (Å^3), symmetries, and bond lengths (pm) for group-12 metal dicarbides in the chain structure. Volume is given with respect to one MC_2 unit. The capital letter after the compound refers to the crystal structures in Fig. 2.

	ZnC_2 (B)	CdC_2 (B)	HgC_2 (B)
Lattice constant a	425.1	438.1	510.5
Lattice constant c	505.2	546.9	529.0
Volume V	45.7	52.5	68.9
Symmetry	$I4/mmm$	$I4/mmm$	$I4/mmm$
	Bond lengths		
Chain-chain dist.	300.6	309.8	361.0
M—C	190.5	211.2	202.9
C—C	124.2	124.5	123.2

TABLE V. Calculated lattice parameters a and c (pm), volumes V (Å^3), symmetries, and bond lengths (pm) for group-2 and -12 metal carbides in the sheet structure. Volume is given with respect to one MC_2 unit. The capital letter after the compound refers to the crystal structures in Figs. 3 and 4.

	Be_3C_6 (E)	Mg_3C_6 (G)	Ca_3C_6 (G)	Sr_3C_6 (G)	Ba_3C_6 (G)	Zn_3C_6 (E)	Cd_3C_6 (E)	Hg_3C_6 (E)
Lattice constant a	390.6	665.0	736.2	782.7	826.2	674.4	715.2	708.2
Lattice constant c	463.2	526.8	543.3	570.0	592.1	711.1	695.1	794.1
Volume V	56.9	67.2	84.9	100.7	116.9	93.4	102.6	115.1
Symmetry	$P\bar{6}2m$	$P\frac{6}{m}mm$	$P\frac{6}{m}mm$	$P\frac{6}{m}mm$	$P\frac{6}{m}mm$	$P\bar{6}2m$	$P\bar{6}2m$	$P\bar{6}2m$
				Bond lengths				
M—C	168.9	214.2	246.2	273.2	280.4	194.8	214.9	212.7
C—C	142.9	142.9	143.2	140.0	141.2	142.6	141.9	140.7

found to be stable, but with slightly higher energies. We emphasize the good agreement between theory and experiment for the M—C and M—N distances of MCN in Table II (M=Cu—Au) and for the lattice constants and M—C distances of MC_2 in Table III.

The difference in the packing geometry of the chain-type dicarbides compared to the packing geometry of the coinage metal cyanides can be understood from the different relative contributions to the interaction forces. Between the monovalent $(Au^+)(CN^-)$ chains, the dispersion forces predominate and one Au^+ is surrounded by six other nominally monopositive Au^+ ions. For the divalent $(M^{2+})(C_2^{2-})$ chains, on the other hand, the Coulomb forces predominate. Hence, in this case the $(M^{2+})(C_2^{2-})$ chains are displaced with respect to each other, so that one M^{2+} ion is surrounded by four C_2^{2-} ions [see Figs. 2(B) and 2(C)]. In support of this, infinite $(M^{2+})(C_2^{2-})$ chains packed into a tetragonal $P4mm$ unit cell [see Fig. 2(A)] were found purely repulsive.

In the search of stable 2D infinite metal dicarbide sheets M_3C_6 (Table V), a similar hexagonal symmetry [Fig. 3(D)], as in the $M_3C_3N_3$ systems [Fig. 1(B′)], was used as a starting point (initially with a large sheet separation). Here, the benzenelike carbon rings are coupled together from the corners by the metal atoms. The calculations in this geometry yielded minimum energy structures for M=Be,Zn—Hg. For the remaining metals, the isolated 2D sheet spontaneously relaxed to a slightly different geometry within the same hexagonal crystal symmetry. The carbon rings rotated 30° with respect to the initial structure to yield the 2D sheet geometry shown in Figs. 4(F) and 4(G). In this structure, the metal atoms are located in the midpoint of the line connecting the C—C edges of every two benzenelike rings. Considering the 3D stacking of these structures, a simple stacking (both rotated and nonrotated cases) was found purely repulsive. Instead, a new 3D packing had to be introduced, where every second sheet was translated by the vector $\vec{v}=(\frac{1}{2}a,\frac{1}{2}a,0)$. For both the structures E and G (see Fig. 4), stable geometries were found.

Figure 5 summarizes the behavior of total energies for the most stable sheets and chains structures. The energy difference ΔE is given for each dicarbide per MC_2 unit; a negative value indicates that the chain structure is preferred. For the experimentally known dicarbides, M=Mg—Ba, the chains are energetically more stable. The energy difference roughly increases following Z, being in all the cases less than 1 eV. Interestingly, for the dicarbides not experimentally known, M=Be, Zn, Cd, and Hg, the sheet structure is predicted to be

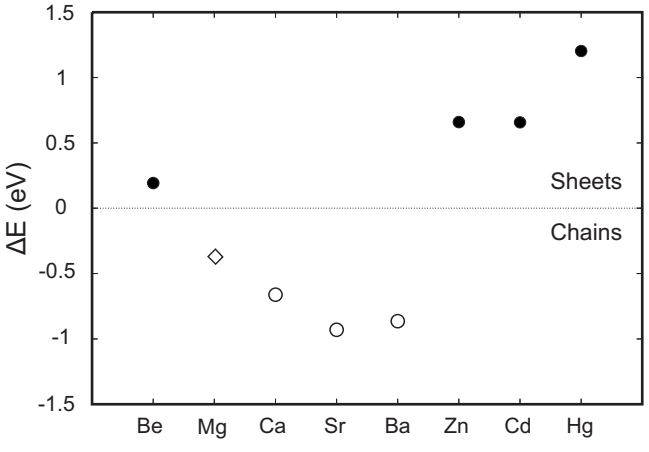

FIG. 5. Total energy differences ΔE (eV) between the most stable chain and sheet structures for group-2 and -12 metal dicarbides: (●) chain B, sheet F; (○) chain B, sheet H; and (◇) chain C, sheet F.

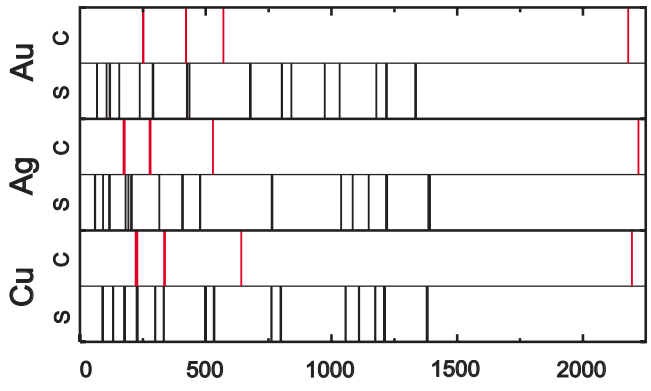

FIG. 6. (Color online) Calculated vibrational frequencies (cm^{-1}) for group-11 metal cyanides at the Γ point. The upper and lower spectra for each metal refer to the chain and sheet structures, respectively. For comparison with experiment, see Table VI.

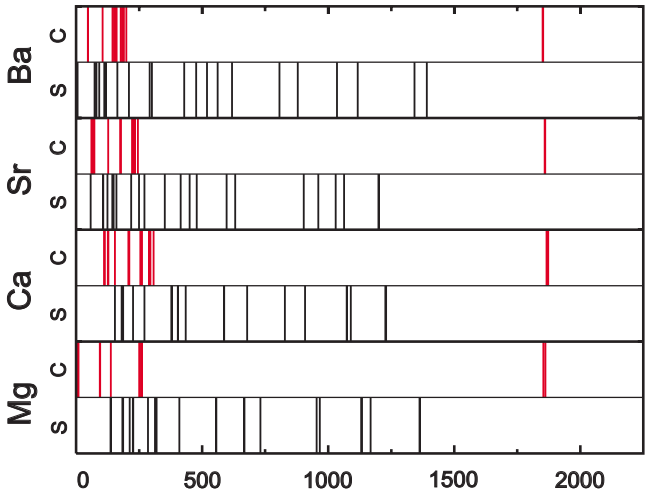

FIG. 7. (Color online) Calculated vibrational frequencies (cm^{-1}) for group-2 metal dicarbides at the Γ point. The upper and lower spectra for each metal refer to the chain and sheet structures, respectively. For comparison with experiment, see Table VII.

the most stable phase, and the energy difference likewise increases roughly following Z.

Even though the vibrational frequencies were calculated only at the center of the Brillouin zone (discussed in Sec. III B), they can provide some hints for the stability of the systems. Most of the chain- and sheet-type dicarbide structures were found to have no or low imaginary frequencies. Notable exceptions are BeC_2 and Be_3C_6, which exhibited imaginary frequencies of the order of $300i$ cm^{-1}, suggesting that the found minimum energy geometry is only a transition state between phases of other symmetry. We did not try to follow the mode to a lower-symmetry minimum. Some imaginary frequencies of the order of $100i$ cm^{-1} were found for chain-type MgC_2, whose structure is, however, in very good agreement with the experiment. Smaller imaginary frequencies (about $50i$ cm^{-1} or smaller) were found for ZnC_2, CdC_2, Ca_3C_6, Sr_3C_6, and Ba_3C_6. We believe that the origin of these imaginary frequencies is related either to the numerical inaccuracies or the anharmonicity of the total energy surface. In fact, small imaginary frequencies have been interpreted in terms of soft mode phonons.[26] It should be noted that for a complete picture of the dynamical stability, one should perform a full phonon band structure calculation.

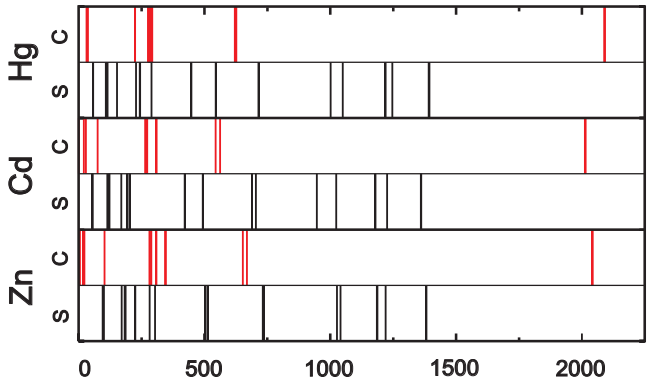

FIG. 8. (Color online) Calculated vibrational frequencies (cm^{-1}) for group-12 dicarbides at the Γ point. The upper and lower spectra for each metal refer to the chain and sheet structures, respectively.

B. Vibrational frequencies

For the cyanide structures, vibrational analysis at the Γ point of the Brillouin zone was performed for isolated chains and isolated sheets, whereas for dicarbides the analysis was done for packed chains and isolated sheets. The rest of the packed structures were not studied because of the difficulties due to the weak chain-chain (for cyanides) and sheet-sheet (for both cyanides and dicarbides) interactions. The frequencies are given in Figs. 6–8 and Tables VI–VIII with compari-

TABLE VI. Experimental and calculated vibrational frequencies (cm^{-1}) for group-11 metal cyanides at the Γ point. For sheets, the four highest frequencies, which correspond to in-plane stretching modes, are reported. The close-lying frequencies have been grouped together.

	CuCN		AgCN		AuCN	
	Calc.	Expt.	Calc.	Expt.	Calc.	Expt.
			Chains			
Stretch (C—N)	2195	2170	2221	2164	2180	2236[a]
Stretch (M—CN)	642	591[a]	529	480[a]	571	598[a]
Bend 1	337,336	326[a]	281,277	272[a]	422,421	358[a]
Bend 2	228,221	168[a]	178,173	112[a]	253,251	224[a]
			Sheets			
	1382,1379		1392,1386		1336,1334	
	1212,1210		1221,1216		1219,1218	
	1174,1109,1057		1174,1087,1039		1178,1032,973	
	799,798		763,762		804,802	

[a]Reference 5.

TABLE VII. Experimental and calculated vibrational frequencies (cm^{-1}) for group-2 and -12 chain-type dicarbides at the Γ point. The highest frequencies, which correspond to stretching modes along the chains, are reported. The close-lying frequencies have been grouped together.

Chains	MgC_2	CaC_2	SrC_2	BaC_2	ZnC_2	CdC_2	HgC_2
Experimental value[a]		1860	1850	1832			
Calculated value	1861,1854	1872,1866	1861,1860	1853,1851	2043,2040	2015,2012	2090,2090
	261,260	308,294	245,234	200,190	669,652	563,545	627,621

[a]Reference 28.

son to available experiments.[5,9–11,25]

Following the assignment by Bowmaker *et al.*[5] for the modes in infinite cyanide chains, it can be seen that the simulation reproduces very well both the vibrational and bending normal modes for the known structures. Here, the two highest modes are the ν(CN) and $\nu(M\mathrm{C/N})$ stretching modes, and the two lowest ones the $\delta(M\mathrm{CN})$ and $\delta(\mathrm{N}M\mathrm{C})$ bending modes. For the known dicarbides in the chain structure, the highest frequencies correspond to the stretching modes and are very close to the experimental ones.

The sheet structures for both cyanides and dicarbides exhibit systematically smaller maximum frequencies compared to those of the chain structures. The higher eigenfrequencies for sheets correspond to in-plane vibrations. Similar to the bending modes in chains, the majority of the lower frequencies in sheets correspond to bending vibrations perpendicular to the plane. For AuCN, the first and second frequencies (Table VI) are close to the in-plane ring deformations of an isolated molecule (1395 and 1208 cm^{-1}) (Ref. 3).

We propose that the possible experimental identification of the sheet-type structures for cyanides could be performed within the range of roughly 650–1500 cm^{-1}. The majority of the in-plane vibrations of the sheets falls into this wavelength region, where no frequencies corresponding to chains interfere. Similarly, the identification of sheet-type dicarbides could be done in the range 700–1800 cm^{-1}, undisturbed by the frequencies of the known chain structures. The frequencies in these ranges correspond mainly to vibrations parallel to the sheets (i.e., parallel to the covalent bonds) and are thus not significantly affected by the DFT deficiences for dispersion. Finally, we note that the local-density approximation (LDA) would typically yield higher frequencies than the GGA.[27] However, the comparison with experiment for stretching modes is rather satisfactory in Tables VI and VII and in some cases a correction toward the LDA could actually worsen the agreement.

C. Band gap and metallicity

The band gap values for the studied systems are reported in Table IX. Since DFT is well known to underestimate the band gaps, one should consider the results as indicative only. However, one can well see the general trends between the geometries and between the elements. In the case of both cyanide and dicarbide chain structures, all the known and predicted one-dimensional (1D) (isolated) and 3D structures are found to be insulators. For the packed 3D dicarbide chain structures, the band gap is largest for HgC_2 (3.7 eV) and smallest for BaC_2 (1.6 eV). The packed chain structures exhibit systematically smaller band gaps than the isolated chains due to the increased overlap of the valence orbitals. The only exception to this picture is BaC_2, which seems to show an opposite trend. All the predicted chain dicarbides (M=Zn—Hg) have larger gaps than the already known chain dicarbides.

For both cyanide and dicarbide 2D (isolated) and 3D sheet structures, the band gaps are clearly smaller than for the chain structures. Packing the sheets in a 3D structure decreases, furthermore, very strongly the band gap value. For dicarbide sheets, we identify two candidates that appear metallic at the present DFT-GGA level of theory: Sr_3C_6 and Ba_3C_6. Both systems may have a significant amount of charge carriers (we find this for both isolated and 3D sheet structures). The rest of the cyanide and dicarbide compounds are found to be either insulators or semimetals with a slight band overlap between the occupied and unoccupied states. In the 3D packed sheet geometry, Zn_3C_6 and Hg_3C_6 have the highest gaps (~0.7 eV). Since the band gap properties are not satisfactorily described by DFT, higher level calculations, such as GW, will be necessary to confirm the present findings especially for Sr_3C_6 and Ba_3C_6.

D. Formation energy of dicarbides M_3C_6

We have estimated the formation energy (E_f) of the predicted dicarbides as the difference between their total energy

TABLE VIII. Calculated vibrational frequencies (cm^{-1}) for group-2 and -12 sheet-type carbides at the Γ point. Only the highest frequencies values, which correspond to in-plane stretching modes, are reported. The close-lying frequencies have been grouped together.

Mg_3C_6	Ca_3C_6	Sr_3C_6	Ba_3C_6	Zn_3C_6	Cd_3C_6	Hg_3C_6
1364,1362	1230,1227	1202,1199	1391,1342	1382,1381	1361,1360	1394,1391
1168	1090,1074	1063,1030	1117,1035	1220	1226	1246
1134,1131	1073	963,901	879,807	1187,1185	1179,1178	1219,1218
966,954	909,828	631	619	1040,1027	1024,947	1050,1001

TABLE IX. HOMO/LUMO band gap (eV) for isolated and packed cyanide and carbide structures. The metallic or semimetallic character is indicated when relevant.

	Chains		Sheets	
	Isolated	Packed	Isolated	Packed
CuCN	3.9	2.5	1.6	0.2
AgCN	4.7	3.1	1.8	0.3
AuCN	4.6	2.3	1.6	0.2
BeC_2	3.6	2.9	0.6	SM[a]
MgC_2	4.2	2.0	1.5	SM
CaC_2	2.6	1.7	SM	SM
SrC_2	2.0	1.7	M[b]	M
BaC_2	1.3	1.6	M	M
ZnC_2	3.9	2.4	1.2	0.7
CdC_2	4.0	2.8	0.6	SM
HgC_2	3.8	3.7	0.9	0.7

[a]Semimetallic.
[b]Metallic.

and the total energy of the corresponding pure elemental metal and graphite:

$$E_f = E(MC_2) - [E(M) + 2E(C)], \quad (1)$$

where $E(MC_2)$ is the total energy of the chain or sheet structure per MC_2 unit. $E(M)$ and $E(C)$ are the total energies of one atom in the zero-temperature phase of the bulk crystal and in graphite, respectively. The total energy for graphite was calculated to be −9.18 eV per atom. The results are given in Table X. As a check of the method, we have also compared the calculated atomization energies for the elemental metals. These values are seen to compare reasonably well with experimental formation enthalpies.

From a thermodynamic consideration, we see that the formation of the dicarbides of Mg and Zn—Hg is clearly endothermic, while CaC_2—BaC_2 are nearly thermoneutral. Note that MgC_2 is 1.19 eV endothermic, compared to the elements, and can only be synthesized from Mg and C_2H_2. On the contrary, MC_2, M=Ca—Ba, are closely thermoneutral and can be prepared directly from the elements. Instead of graphite, which is a highly stable material, one could think of different benzene-derived substances as possible starting materials in the synthesis of the predicted sheet-type compounds.

Although the linear C—M(II)—C bonding system is well known, for instance, in $Hg(CH_3)_2$ or $Hg(C_6H_5)_2$, they are here grouped to nominal oxidation states of M^{2+} and C_6^{6-}. The latter is previously unknown.

TABLE X. Formation energies E_f for group-2 and group-12 carbides and the corresponding difference $\Delta E_f = E_f(MC_2) - E_f(M_3C_6)$, per MC_2 unit. The calculated atomization energy $E_{at}(M)$ and the experimental atomization enthalpy $H_{at}(M)$ for the pure solid metals are given as a technical test. All values are in eV.

M	$E_f(MC_2)$	$E_f(M_3C_6)$	ΔE_f	$E_{at}(M)$	$H_{at}(M)$[a]
Mg	1.19[b]	1.55	−0.36	1.51	1.531
Ca	−0.04[b]	0.61	−0.65	1.91	1.847
Sr	0.01[b]	0.92	−0.91	1.61	1.704
Ba	0.20[b]	1.05	−0.85	1.88	1.866
Zn	2.66	1.99	0.67	1.11	1.355
Cd	2.97	2.32	0.65	0.72	1.161
Hg	3.20	1.99	1.21	0.08	0.635

[a]Experimental value (Ref. 29).
[b]Compound experimentally known.

IV. CONCLUSIONS

We have suggested a number of solid substances, of which the sheet-type $M_3C_3N_3$ (M=Cu, Ag, Au) and the sheet-type M_3C_6 (M=Mg—Ba) may have the best chance of being prepared. The density of these substances is in general lower than that of the known chain-type structures. For the identification of these substances, we have reported their geometries and vibrational frequencies at the Γ point of the Brillouin zone. The majority of the in-plane frequencies of these compounds are clearly separated from the stretching and bending frequencies of the known chain-type cyanide and dicarbide structures. Evidence is found that the Sr and Ba sheet-type compounds are metallic both in the 3D crystal and as isolated sheets at the present DFT-GGA level of theory. All group-2 or group-12 sheet-type structures are endothermic. The least endothermic one is calcium carbide. If any of these compounds can be made, the metallic Sr and Ba ones may find the most interesting applications. As these structures have a very different geometry from the corresponding known ones, a controlled synthesis from appropriate starting materials is necessary. The phase formation kinetics plays a crucial role since most of these structures have similar or slightly higher formation energies. The sheet structures of lanthanides might form a further possible class of compounds. Note that insulating or metallic LnC_2 with a CaC_2 structure are known for Ln=Y, La, Ce, Tb, Yb, Lu, and U.[30]

ACKNOWLEDGMENTS

We would like to thank Uwe Ruschewitz for useful comments. We belong to the Finnish Center of Excellence in Computational Molecular Science (2006–2011). Grants Nos. 110571, 200903, 201291, 205967, and 206102 of The Academy of Finland are also gratefully acknowledged. The work was also supported by the Research Funds of the University of Helsinki.

*Author to whom correspondence should be addressed; pekka.pyykko@helsinki.fi

[1] L. Gagliardi, Theor. Chem. Acc. **116**, 307 (2006).
[2] G. S. Zhdanov and E. A. Shugam, Zh. Fiz. Khim. **19**, 519 (1945).
[3] M. O. Hakala and P. Pyykkö, Chem. Commun. (Cambridge) **2006**, 2890.
[4] M. I. Katsnelson, K. S. Novoselov, and A. K. Geim, Nat. Phys. **2**, 620 (2006).
[5] G. A. Bowmaker, B. J. Kennedy, and J. C. Reid, Inorg. Chem. **37**, 3968 (1998).
[6] S. J. Hibble, S. M. Cheyne, A. C. Hannon, and S. G. Eversfield, Inorg. Chem. **41**, 1042 (2002).
[7] S. J. Hibble, S. M. Cheyne, A. C. Hannon, and S. G. Eversfield, Theor. Chem. Acc. **41**, 4990 (2002).
[8] R. W. Henn, C. Bernhard, R. K. Kremer, T. Gulden, A. Simon, T. Blasius, and C. Niedermayer, Phys. Rev. B **62**, 14469 (2000).
[9] P. Karen, A. Kjekshus, Q. Huang, and V. L. Karen, J. Alloys Compd. **282**, 72 (1999).
[10] V. Vohn, M. Knapp, and U. Ruschewitz, J. Solid State Chem. **151**, 111 (2000).
[11] V. Vohn, W. Kockelmann, and U. Ruschewitz, J. Alloys Compd. **284**, 132 (1999).
[12] U. Ruschewitz, Coord. Chem. Rev. **244**, 115 (2003).
[13] E. Ruiz and P. Alemany, J. Phys. Chem. **99**, 3114 (1995).
[14] G. Kresse and J. Hafner, Phys. Rev. B **47**, 558 (1993).
[15] G. Kresse and J. Furthmüller, Comput. Mater. Sci. **6**, 15 (1996).
[16] G. Kresse and J. Furthmüller, Phys. Rev. B **54**, 11169 (1996).
[17] P. E. Blöchl, Phys. Rev. B **50**, 17953 (1994).
[18] G. Kresse and D. Joubert, Phys. Rev. B **59**, 1758 (1999).
[19] J. Paier, R. Hirschl, M. Marsam, and G. Kresse, J. Chem. Phys. **122**, 234102 (2005).
[20] J. P. Perdew, K. Burke, and M. Ernzerhof, Phys. Rev. Lett. **77**, 3865 (1996).
[21] S. J. Hibble, A. C. Hannon, and S. M. Cheyne, Inorg. Chem. **42**, 4724 (2003).
[22] G. Herzberg and J. W. T. Spinks, Z. Phys. **91**, 386 (1934).
[23] P. Pyykkö, S. Riedel, and M. Patzschke, Chem.-Eur. J. **11**, 3511 (2005).
[24] B. Zibrowius, C. Bähtz, M. Knapp, and U. Ruschewitz, Phys. Chem. Chem. Phys. **6**, 5237 (2004).
[25] M. Knapp and U. Ruschewitz, Chem.-Eur. J. **7**, 874 (2001).
[26] M. Sternik and K. Parlinski, J. Chem. Phys. **122**, 064707 (2005).
[27] F. Favot and A. Dal Corso, Phys. Rev. B **60**, 11427 (1999).
[28] O. Reckeweg, A. Baumann, H. A. Mayer, J. Glaser, and H.-J. Meyer, Z. Anorg. Allg. Chem. **625**, 1686 (1999).
[29] D. R. Lide, *CRC Handbook of Chemistry and Physics* (CRC Press, Boca Raton, FL, 1999).
[30] M. Atoji, J. Chem. Phys. **35**, 1950 (1961).